This file contains all reviewer reports in order by version, followed by all author rebuttals in order by version.

nature portfolio

Peer Review File

Organic Phosphorescence in Pt(II)-Complexes linked to Organic Chromophores for Blue-Emitting Organic Light-Emitting Diodes

Corresponding Author: Professor Ho-Jin SON

Version 0:

Reviewer comments:

Reviewer #1

(Remarks to the Author)
Recommendation: This paper is publishable with minor revision.
Comments: The manuscript describes a thorough study on a type of Pt(II) complexes linked with organic luminophores. The manuscript is well written, and the results are presented in a clear form. The series of Pt(II) complexes exhibit dual emission bands with TTET process. The authors provided details with reliable experimental data, and gave convincing explanation for the TTET mechanism. The presents of mechanism investigation are contemporarily important for the exploration on application-specific phosphorescent emitters. However, in the introduction of the manuscript, this paper overly emphasizes some academic hotspots that seem to have correlations with the research of the manuscript. This may mislead the reader. In review of the whole paper for publication, the authors are required to address the following questions:
1) The section of introduction should be rewritten. The whole research on Pt(II) complexes are traditional phosphorescent materials, which are distinct from the concept of organic persistent room-temperature phosphorescence (OPRTP) or afterglow materials. Moreover, the authors also should refer to the previous work on dual phosphorescence, such as Inorg. Chem. 2016, 55, 3829–3843, Materials Chemistry and Physics 162 (2015) 822-830, Chem. Eur.J. 2020, 26,11307 –11315, and etc.
2) In PL in figure 3 as well as the EL in Figure 11, the phosphorescence form Pt center is quenched by the Cz or Np appendage. The authors attribute this to TTET enhancements from the suppression of non-radiative transitions. This is a crude explanation, and one reason of 3MLCT suppression cannot be excluded. Otherwise, the TTET of solid state sample can be fitted by the measurements of transient absorption.
3) Based on the lifetime data of Supplementary Table 6, the phosphorescent transition of both 3MLCT and 3LC are much faster than traditional phosphorescent materials, normally with the lifetimes of 10-6 S-1 level. Can you give some reasonable explanations?
4) The lifetimes data on the main emission peaks of the sample in PMMA are needed, and comments on comparing the data with those of the sample in solutions are required.
5) In the methods of synthesis section, the data of 13C NMR should be presented for the structure characterizations.

Reviewer #2

(Remarks to the Author)
The authors, S. W. Jeong, H. J. Lee, T. Kim, C. H. Kim, H.-J. Son et al., reported on the novel four-coordinate N-heterocyclic carbene Pt(II) complexes bearing carbazole or naphthalene group showing exothermic triplet-triplet energy transfer, in particular persistent organic phosphorescence of organic molecules under ambient conditions. The results of this paper look like giving an insight to corresponding researcher for luminescent materials in both the academic and optoelectronic industrial fields. The approach for the purpose of this work was also well designed. The description for the Introduction section well focused on this research scoop and the added reference papers look proper. In this regard, the reviewer would like to recommend that the manuscript would be suitable for publication to Communications Chemistry as an Article. However, there are the parts which the authors should revise the manuscript and thoroughly consider as the following:
1. Figure 1: It would be helpful to either indicate the dihedral angle or demonstrate the orthogonality between the ligand and substituent.
2. Line #154: The text describes 312 nm, but Table 1 lists it as 313 nm. Harmonizing such numerical discrepancies would enhance readability. Review and correct similar instances throughout the manuscript if any.
3. Figure 3 (middle): The PL data for Pt(PI)(acac)+Cz and Pt(PI)(acac)+Np suggest fluorescence from Cz or Np and phosphorescence from Pt(II) (line #193 and #201). However, the graph shows a slight shoulder peak for Pt(PI)(acac)+Np,

while phosphorescence is not convincingly observed for Pt(PI)(acac)+Cz. Please clarify this inconsistency.
4. Line #236~: The statement that “the PL excitation spectra of both Pt-Cz and Pt-NP show distinct bands in the 340–400 nm range” does not align with the data in Supplementary Figure 8. Apart from Pt-Cz’s very weak absorption (λem = 450 nm, green line), no clear data supports this range. Please address this discrepancy.
5. Page 13, Line #251: The excimer emission is described as appearing at 50 μM, which seems unexpectedly dilute. While Pt-Np’s behavior at 1 μM is somewhat understandable, excimer emission attributed to Pt-Pt interaction (Line #251) suggests that Pt-Cz might also exhibit this phenomenon. Additional experiments, such as PL measurements at high concentrations (above mM) or in the crystalline state, could be helpful. Molecular interaction data from unit cell analyses of Pt-Np and Pt-Cz crystals would strengthen this discussion.
6. Page 13, Figure 4 & Supplementary Figure 9: The criteria for selecting the wavelengths for time-profile measurements are unclear. For example, Fig. 2 shows emission wavelengths corresponding to Pt-Cz and the excimer peak for 1 μM Pt(PI)(acac). However, other cases feature measurements at ambiguous wavelengths, such as near PL valleys. Consider either unifying the criteria or providing a clear explanation.
7. Figure 4 (top): Include an explanation of the data, and clarify the meaning of the blue-to-yellow color gradient with appropriate labels.
8. Page 25, Supplementary Table 7: The increase in CIEy and EL emission wavelengths with higher dopant concentrations seems related to Pt-Cz excimer formation, as discussed in Line #452. This aligns with the questions #5, suggesting the need for additional experiments.
9. Thermal stability: Since device testing was performed, additional TGA experiments to analyze thermal stability and decomposition characteristics would be beneficial.
10. Figures 8 & 2: The absorption spectra in Fig. 2 suggest that Pt-Cz’s vertical excitation is similar to Cz, while Pt-Np resembles Pt(II). This implies that Fig. 8a’s vertical excitation for Pt-Cz might terminate at 1[Cz]* rather than 1MLCT. What is the authors’ perspective on this?
11. Figure 8: Despite both molecules having the same TTET mechanism, the final emission lifetimes differ significantly (24 ns vs. >100 μs). A more detailed explanation is needed for this discrepancy. Is there any some examples previously reported?
12. Molecular design: Cz is located at the para position of phenyl, while Np is at the ortho position. Since the electronic environments differ, provide an explanation of the rationale and implications of these molecular designs.
13. Figure and Table descriptions: The explanations for figures and tables are insufficiently detailed, making it difficult to connect them with the text. Use clear symbols (a, b, etc.), and add detailed descriptors such as left, right, middle, top, and bottom in figure legends to enhance clarity.
14. The originality of this study, Line #69~: While the need for developing novel OPRTP materials without SOC via heavy atom effects is acknowledged, the manuscript ultimately relies on Pt to utilize SOC for TTET. This raises a question about the novelty of the approach. Address this concern.

Minor points
- Supplementary Scheme 1: Replace (v) with (iv) in the explanation section.
- Supplementary Figures 9 and 10: The concentration unit is incorrect; revise from mM to μM.
- Line #219: The footnote in Table 1 mentions 3 wt% PMMA, whereas the text specifies 5 wt%. Provide a clear and consistent description.

Version 1:

Reviewer comments:

Reviewer #1

(Remarks to the Author)
The author provided a detailed response to the question in thir revised manuscript. All the concerns have been well addressed, and the paper looks quite convincing in their presented TTET mechanism. In this view, this manuscript can be published without any further revision.

Reviewer #2

(Remarks to the Author)
The authors have thoroughly addressed the reviewer's comments with various experimental evidence, leading to significant improvements and an overall enhancement of the manuscript's quality. Therefore, I recommend the publication of this paper in its revised form.

Reviewer: 1

Recommendation: This paper is publishable with minor revision.

Comments: The manuscript describes a thorough study on a type of Pt(II) complexes linked with organic luminophores. The manuscript is well written, and the results are presented in a clear form. The series of Pt(II) complexes exhibit dual emission bands with TTET process. The authors provided details with reliable experimental data, and gave convincing explanation for the TTET mechanism. The presents of mechanism investigation are contemporarily important for the exploration on application-specific phosphorescent emitters. However, in the introduction of the manuscript, this paper overly emphasizes some academic hotspots that seem to have correlations with the research of the manuscript. This may mislead the reader. In review of the whole paper for publication, the authors are required to address the following questions:

Q1-1. *The section of introduction should be rewritten. The whole research on Pt(II) complexes are traditional phosphorescent materials, which are distinct from the concept of organic persistent room-temperature phosphorescence (OPRTP) or afterglow materials. Moreover, the authors also should refer to the previous work on dual phosphorescence, such as Inorg. Chem. 2016, 55, 3829−3843, Materials Chemistry and Physics 162 (2015) 822-830, Chem. Eur.J. 2020, 26,11307 –11315, and etc.*

A1-1. As per the reviewer's request, we have revised the introduction, incorporating references to previous studies on the dual phosphorescence of heteroleptic transition metal complexes. The revised introduction part reads "*On the other hand, blue phosphorescence from organic units can be efficiently achieved through intramolecular triplet-triplet energy transfer (TTET).*[20-23] *This process occurs when the triplet-excited state of a heavy-atom-containing transition metal complex transfers energy to the lower-lying triplet state of a tethered organic unit. Recent studies have demonstrated that Ir(III) complexes with two cyclometallating ligands of different energy levels (L = higher-energy ligand; L' = lower-energy ligand) can exhibit dual emissions.*[24-28] *These emissions arise from the higher-energy triplet metal-to-ligand charge transfer (*^{3}*MLCT) state and the lower-energy triplet ligand-centered (*^{3}*L'C) state, respectively. Notably,* ^{3}*L'C emission, observed as room-temperature organic phosphorescence, results from intramolecular TTET between the* ^{3}*MLCT and* ^{3}*L'C states at close proximity within the ligands bound to the Ir metal center. This TTET process is exothermic, driven by the energy difference between the high-lying* ^{3}*MLCT and low-lying* ^{3}*L'C states, leading to efficient ligand-centered triplet emission. Thus, positioning an organic moiety near a high triplet energy metal-coordinated ligand facilitates efficient TTET from the donor's higher triplet state to the acceptor's lower triplet state, amplifying phosphorescence from the organic luminophore. This approach provides an effective strategy for enhancing triplet emission from various organic compounds. Among various organic luminophores, Cz derivatives exhibit versatile utility for a range of organic electronics including OLEDs owing to their high quantum yields (Φ) and stability.*[13,18,29] *Notably, Cz derivatives have recently emerged as crucial building blocks in host/dopant systems and TADF materials for blue-emitting OLEDs.*[13,18] *However, the contribution of the phosphorescence quantum yield (*Φ_P*) to the overall Φ remains minimal.*[30] *The lowest triplet excited state of Cz derivatives, characterized by a pure* $^3(\pi,\pi^*)$ *configuration, has been shown to deliver persistent lifetimes.*[31,32] *However, because their triplet energy level is relatively high (*$T_1 \approx 3.0$ *eV), Cz derivatives are primarily used as host materials in the emitting layers of multi-layered OLEDs, rather than as emissive materials themselves.*[3,4] *Although an example of organic persistent room-temperature phosphorescence (OPRTP) using a Cz unit via intramolecular TTET has been reported, the OPRTP is only observed in the crystal or condensed phase.*[33] *This phase exhibits a significant redshift in the emission band to longer wavelengths (*$\lambda_p \approx 500–700$ *nm), contrasting with the low-temperature emission of isolated Cz units (*$\lambda_{p,77\,K} \approx 480$ *nm). These properties hinder processability and limit practical applications, especially as a blue-emitting material.*[34-37]".

Q1-2. *In PL in figure 3 as well as the EL in Figure 11, the phosphorescence from Pt center is quenched by the Cz or Np appendage. The authors attribute this to TTET enhancements from the suppression of non-radiative transitions. This is a crude explanation, and one reason of* ^{3}*MLCT suppression cannot be excluded. Otherwise, the TTET of solid state sample can be fitted by the measurements of transient absorption.*

A1-2. We thank the reviewer for the valuable comment. As stated in our initial submission, the significant enhancement of ^{3}LC emission in solid **Pt-Cz** and **Pt-Np** compared to the solution phase is attributed to a substantial improvement in TTET efficiency between the Pt core and the organic tethers. As the reviewer correctly pointed out, we currently have no direct evidence for the enhanced quenching of ^{3}MLCT emission from the Pt core in the PMMA film and EL device

via accelerated TTET process. To address this issue, we recorded steady-state PL spectra of the **Pt-Cz** and **Pt-Np** solutions with varying concentrations (see Supplementary Figure 12 below) and also performed additional TRPL experiments for the films (PMMA 5 wt%) and crystalline samples. (Supplementary Figure 13-14 and Table 7). It should be noted that for **Pt-Cz** in solution, the PL intensity ratio between the Pt core (^{3}MLCT) and the organic tether (^{3}LC) was highly dependent on its concentration. Specifically, the PL lifetime of ^{3}LC state was ~24 ns in the solution (50 μM), but increased significantly (>850 ns) in the glassy PMMA matrix (5 wt%), as described in our response to the reviewer's question (***Q1-4***). That is, flexible skeletal motions of **Pt-Cz** in the excited state, which lead to rapid deactivation of the ^{3}LC state, are responsible for the short lifetime observed in the solution. These fast non-radiative pathways can be effectively suppressed in the glassy polymer matrix. This experimental evidence suggests that the enhanced PL intensity of ^{3}LC state in the PMMA and OLED films, along with negligible ^{3}MLCT emission, primarily originates from the prolonged lifetimes of the ^{3}LC state. Thus, it is reasonable to conclude that the significantly enhanced PL intensity of ^{3}LC in the EL device is mainly due to the activation of the ultrafast TTET process, combined with the restricted skeletal motions of **Pt-Cz** embedded in the glassy thin film. While the rate of the TTET process may also be affected by the structural confinement in the polymer matrix, further confirmation would require ultrafast TA experiments on film samples. However, under our current experimental conditions, such analysis is challenging due to strong scattering light from non-transparent thin film, and significant photodamage to the Pt(II) based solid samples during the measurements. This issue will be addressed in a future study using an improved measurement setup.

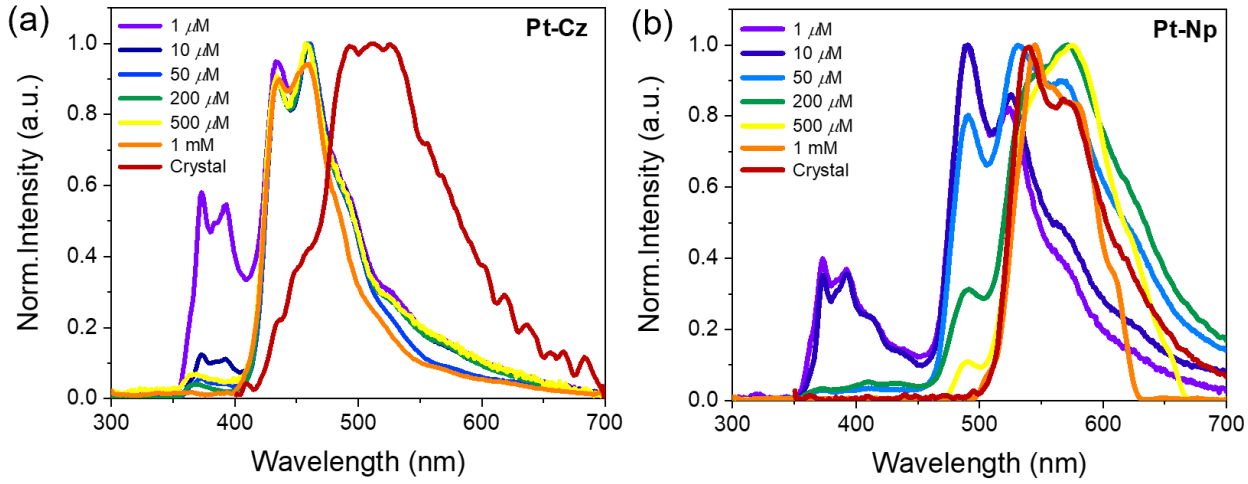

Supplementary Figure 12. Steady-state emission spectra of (a) **Pt-Cz** and (b) **Pt-Np** across a wide range of solution concentrations (1 μM to 1 mM) and in the crystalline state.

(Revision in manuscript)

On pages 12-13 and 17-18, revised the following paragraph.

The revised text reads "*Interestingly, as shown in Table 1, the solidified Pt(II) complexes (5 wt% in poly(methyl methacrylate) (PMMA) polymer films) exhibited significantly improved emission efficiencies (Φ_{em}) compared to those obtained in solution at 300 K. Additionally, unlike the dual emission (^{3}MLCT and ^{3}LC) observed in the solution phase, the rigidified Pt(II) complexes in the PMMA film predominantly exhibited ^{3}LC emissions from the Cz or Np moiety with minimal ^{3}MLCT emission from the core Pt^{II}(PI)(acac) complex (Fig. 3e and 3f). This may indicate a substantial improvement in the TTET efficiency from the ^{3}MLCT state of the core Pt(II) site to the ^{3}LC state of the organic peripheral groups and/or the activation of the ultrafast TTET process followed by prolonged population relaxations of the product ^{3}LC state in the glassy polymer film. This hypothesis was further verified with the time-resolved optical spectroscopy results (vide infra). (…) The PL intensity ratio between the ^{3}MLCT (~375 nm) and ^{3}LC (465 nm) states for **Pt-Cz** in solution was also sensitive to its concentration (Supplementary Figure 12a). The PL intensity of the Pt core (^{3}MLCT) was moderate in the diluted solution (1 μM), but highly diminished in concentrated solutions above 50 μM, resulting in the relatively strong PL spectrum of the TTET-induced ^{3}[Cz]*. Similarly, the PMMA film (5 wt%) also exhibited strong ^{3}LC emission with negligible ^{3}MLCT one (Fig. 3e). Note that the PL lifetime of the ^{3}LC state at 450 nm was 4.7 ns (~80% in amplitude), 24.2 ns for the dilute (1 μM) and concentrated (50 μM) solutions, respectively, and increased significantly*

*(>850 ns) in the polymer matrix (Supplementary Figures 13-14 and Tables 6-7). These experimental results suggest that the enhanced PL intensity of the ^{3}LC state in the thin film, along with negligible ^{3}MLCT emission, primarily arises from the prolonged lifetimes of the ^{3}LC state (additionally, the TTET process may be partially affected by the structural confinement in the polymer matrix). That is, flexible skeletal motions of **Pt-Cz** in the excited state, which lead to rapid deactivation of the ^{3}LC state, are responsible for the short lifetime observed in the diluted solution. These fast non-radiative pathways can be effectively suppressed in the glassy polymer matrix. Accordingly, in the concentrated solution (50 μM), the solvated **Pt-Cz** may experience weak conformational confinements from long-range intermolecular interactions, leading to the disappearance of the fast decay component (~4.7 ns).*"

Q1-3. *Based on the lifetime data of Supplementary Table 6, the phosphorescent transition of both ^{3}MLCT and ^{3}LC are much faster than traditional phosphorescent materials, normally with the lifetimes of 10^{-6} S^{-1} level. Can you give some reasonable explanations?*

Q1-4. *The lifetimes data on the main emission peaks of the sample in PMMA are needed, and comments on comparing the data with those of the sample in solutions are required.*

A1-3 and A1-4. To address these comments, we performed additional TRPL spectra measurements for the samples in PMMA (5 wt%) and crystalline forms. Supplementary Figures 13 and 14 present the TRPL spectra (raw images) and their corresponding time-profiles at selected detection wavelengths. Multiexponential fitting results for the TRPL profiles are listed in Supplementary Table 7. Additionally, Supplementary Figure 11 and Table 6 includes the TRPL results of **Pt-Cz** in a diluted solution (1 μM).

(Revision in manuscript)

On pages 16-19, we have fully rewritten the section titled "TTET dynamics probed by time-resolved optical spectroscopy". The updated parts read "*To systematically investigate the excimer formations of **Pt-Cz** and **Pt-Np** in solution, the steady-state PL spectra of the two samples were recorded with varying concentrations (1 μM ~ 1 mM) (Supplementary Figure 12). For comparison, steady-state PL spectra of their crystalline forms were also recorded to get insights into excimer formation in extended oligomeric aggregates. **Pt-Cz** solutions displayed nearly identical emission features around 465 nm (^{3}LC) with negligible excimer band at 570 nm across a wide concentration range (1 μM to 1 mM). The fully red-shifted excimer band was observed only in its crystalline state. The predominant generation of the ^{3}[Cz]* state in solution indicates that the perpendicular geometry of the appended Cz moiety effectively prevents intermolecular stacking interactions even in the highly concentrated solution (>50 μM). Consequently, the apparent red-shifted PL band by the ultrafast TTET process can be exclusively observed in **Pt-Cz,** as shown in Fig. 4c. On the other hand, the short PL lifetime of ~24 ns at 465 nm (see Supplementary Table 6) indicates that flexible skeletal motions of **Pt-Cz** in the excited state cause rapid non-radiative relaxations of the ^{3}[Cz]* state.[39] This is further supported by the prolonged PL lifetime of the ^{3}LC state in a glassy polymer matrix (vide infra). The strong intermolecular interactions in **Pt-Np** are further corroborated by the pronounced change in the excimer band with increasing concentration and its resemblance to the single PL band at 570 nm observed in the crystalline state. That is, the Np group plays a key role in inducing more rigid and extended H-type molecular aggregates in solution. In this context, the formation of the well-stacked aggregates should be responsible for the prolonged PL lifetimes (>100 μs) of both ^{3}LC and excimer states in the concentrated solution (50 μM) (Fig. 4f).*

The photophysical properties of the Pt core, Pt^{II}(PI)(acac), were further examined in PMMA thin film and crystalline form using TRPL spectra measurements (Supplementary Figuires 13-14 and Table 7). In the PMMA film (5 wt%), the excimer emission at 550 nm was not discernible even in the time-domain measurement, which is consistent with the steady-state spectrum shown in Fig. 3e. The TRPL profile of the thin film at 450 nm revealed diverse population relaxations, including an additional slow decay component of 3.41 μs, whereas the diluted solution (1 μM) showed a monotonic PL decay (1.1 μs) with negligible spectral change (Supplementary Table 6-7). This suggests that Pt^{II}(PI)(acac) monomers are more likely to be isolated within the PMMA matrix, and some conformers become further rigidized to give the longer PL lifetime. In the crystalline phase, the sample exhibits the apparent excimer band at 550 nm with diverse population decays exceeding 25 μs, similar to the observations in the concentrated solution (50 μM, see Supplementary Figure 11b). Thus, we conclude that the low dopant concentration of 5 wt% in the PMMA matrix is insufficient to facilitate the formation of Pt^{II}(PI)(acac) excimers. Instead, well-stacked oligomeric aggregates are more favorable in the concentrated solution (50 μM) and crystalline form.

*The PL intensity ratio between the ^{3}MLCT (~375 nm) and ^{3}LC (465 nm) states for **Pt-Cz** in solution was also sensitive to its concentration (Supplementary Figure 12a). The PL intensity of the Pt core (^{3}MLCT) was moderate in the diluted solution (1 μM), but highly diminished in concentrated solutions above 50 μM, resulting in the relatively strong PL spectrum of the TTET-induced ^{3}[Cz]*. Similarly, the PMMA film (5 wt%) also exhibited strong ^{3}LC emission with negligible ^{3}MLCT one (Fig. 3e). Note that the PL lifetime of the ^{3}LC state at 450 nm was 4.7 ns (~80% in amplitude), 24.2 ns for the dilute (1 μM) and concentrated (50 μM) solutions, respectively, and increased significantly (>850 ns) in the polymer matrix (Supplementary Figures 13-14 and Tables 6-7). These experimental results suggest that the enhanced PL intensity of the ^{3}LC state in the thin film, along with negligible ^{3}MLCT emission, primarily arises from the prolonged lifetimes of the ^{3}LC state (additionally, the TTET process may be partially affected by the structural confinement in the polymer matrix). That is, flexible skeletal motions of **Pt-Cz** in the excited state, which lead to rapid deactivation of the ^{3}LC state, are responsible for the short lifetime observed in the diluted solution. These fast non-radiative pathways can be effectively suppressed in the glassy polymer matrix. Accordingly, in the concentrated solution (50 μM), the solvated **Pt-Cz** may experience weak conformational confinements from long-range intermolecular interactions, leading to the disappearance of the fast decay component (~4.7 ns).*

*The excited state dynamics of **Pt-Np** in condensed phase was highly complicated by the formation of molecular aggregates facilitated by the organic tether moieties (Supplementary Figures 13-14 and Tables 6-7). As shown in Fig. 4b, the **Pt-Np** solution revealed the strong ^{3}LC and excimer emissions due to effective stacking interactions in the aggregates. Notably, the PL lifetimes of both ^{3}LC and excimer states were rather longest (> 100 μs) in the concentrated solution (50 μM) than in the crystalline form. In the crystal, the PL lifetime of the ^{3}LC state at 475 nm was ~250 ns, while the 2nd and 3rd time constants (10~16 μs) were attributed to spectral overlap of the strong excimer emission at 600 nm. This is in sharp contrast to **Pt-Cz**, where the ^{3}[Cz]* product in solution undergoes the relatively fast deactivation (~24 ns) compared to that in the solid-state samples. According to the packing structure of **Pt-Np** crystal in Fig. 3d, the herringbone arrangements of fully-stacked **Pt-Np** dimeric units in the crystal may impede strong excitonic interactions across the extended spatial domain. In this context, we argue that extended H-type molecular aggregates with a long coherence length are favorable in solution, thereby reducing oscillator strengths of the optical transitions and suppressing structural distortions. It is noteworthy that the spectral width of the excimer PL band at 570 nm gradually decreased with increasing concentration (Supplementary Figure 12b), implying that effective and extended stacking interactions in solution promote the formation of a well-ordered aggregate with reduced conformational disorder. On the other hand, in the PMMA film (5 wt%), the PL lifetime at 475 nm was similar to that at 600 nm, and only an extremely weak PL with a time-constant of 230 μs was detected at 600 nm (Supplementary Table 7), indicating negligible excimer emission. Again, this confirms that the dopant concentration of 5 wt% is sufficiently low to minimize excimer formation in the thin film.*

*The excimer formation kinetics of **Pt-Np** in the concentrated solution (50 μM) and crystalline form can be exclusively resolved at the red-side of the PL band (λ_{em} = 600 nm) (Fig. 4f and Supplementary Figure 14). In solution, the TTET process occurs instantaneously (limited by the IRF), but the excimer formation appears to be a delayed dynamic process of molecular excitons, as evidenced by the slow rise component of 17.9 μs at 600 nm (Supplementary Table 7). The origin of the slow-rise is unclear but may be associated to the excitonic dynamics occurring in the highly extended oligometric aggregates with conformational heterogeneities because the crystalline form rather showed a relatively fast rise of 1.82 μs. Further experiments are currently underway to elucidate the slow excitonic dynamics of **Pt-Np** in these extended systems.*".

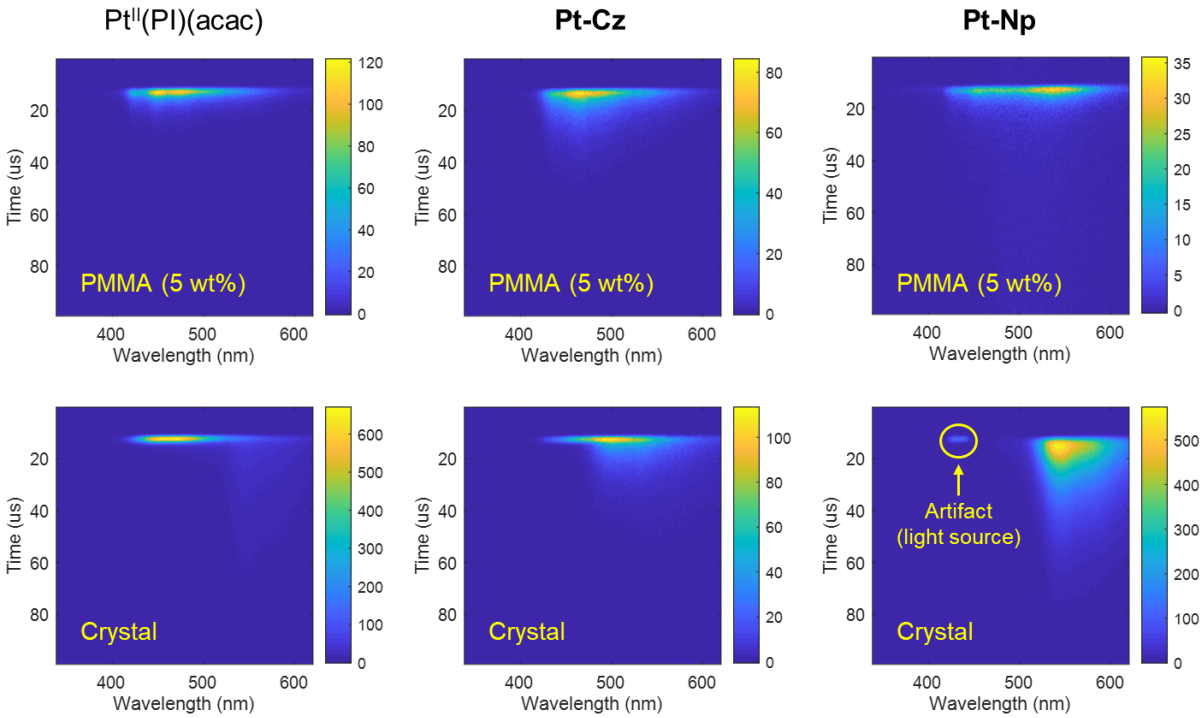

Supplementary Figure 13. Time-resolved photoluminescence spectra (raw contour images) of Pt^{II}(PI)(acac), **Pt-Cz**, and **Pt-Np** in PMMA film (5 wt%) and crystalline forms. The vertical colorbar represents the PL intensity in counts per second (cps).

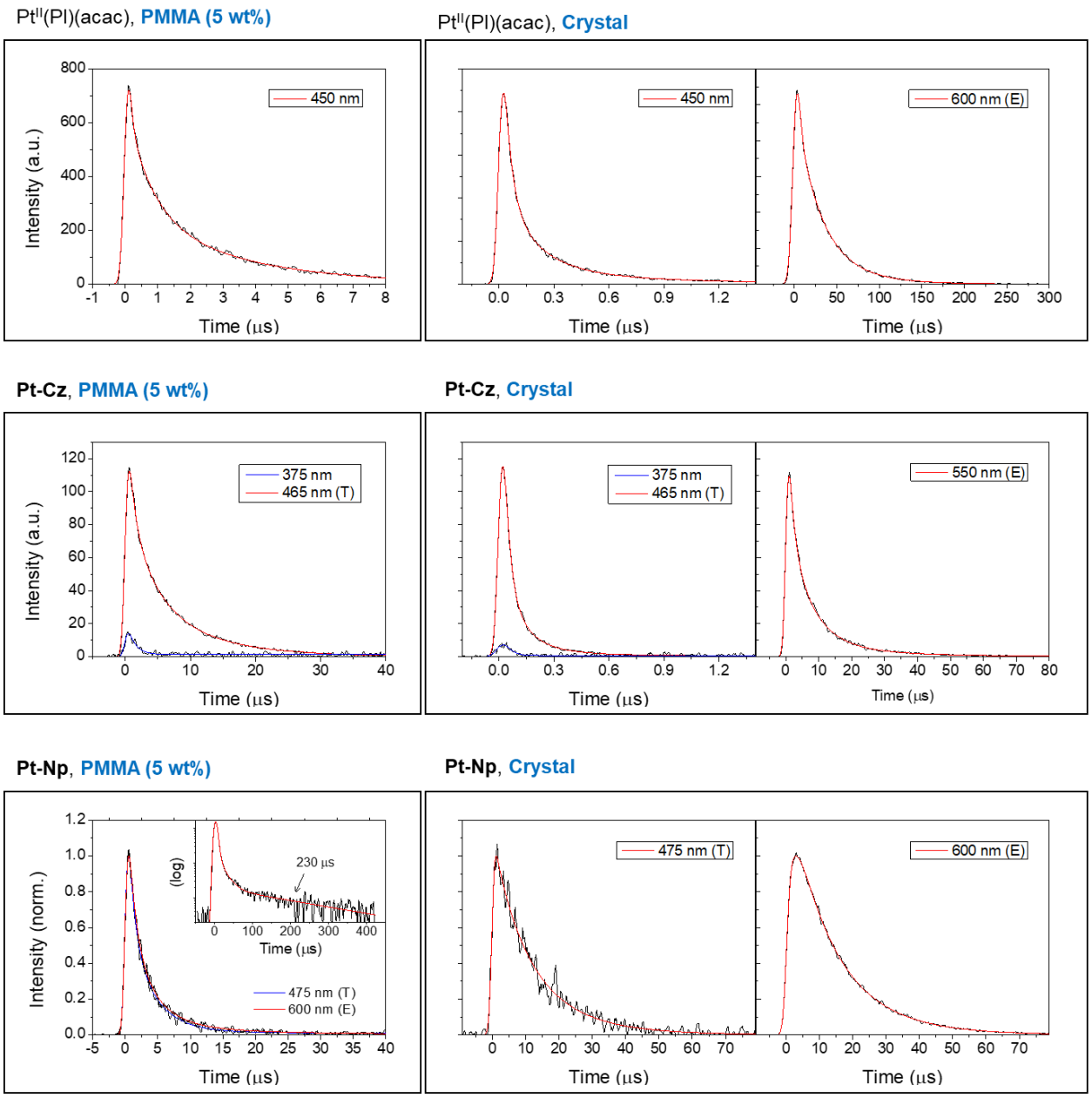

Supplementary Figure 14. Time-resolved photoluminescence profiles of Pt^{II}(PI)(acac), **Pt-Cz**, and **Pt-Np** in PMMA film (5 wt%)and crystalline forms. The symbols T and E in legend denote TTET (^{3}LC) and Excimer, respectively.

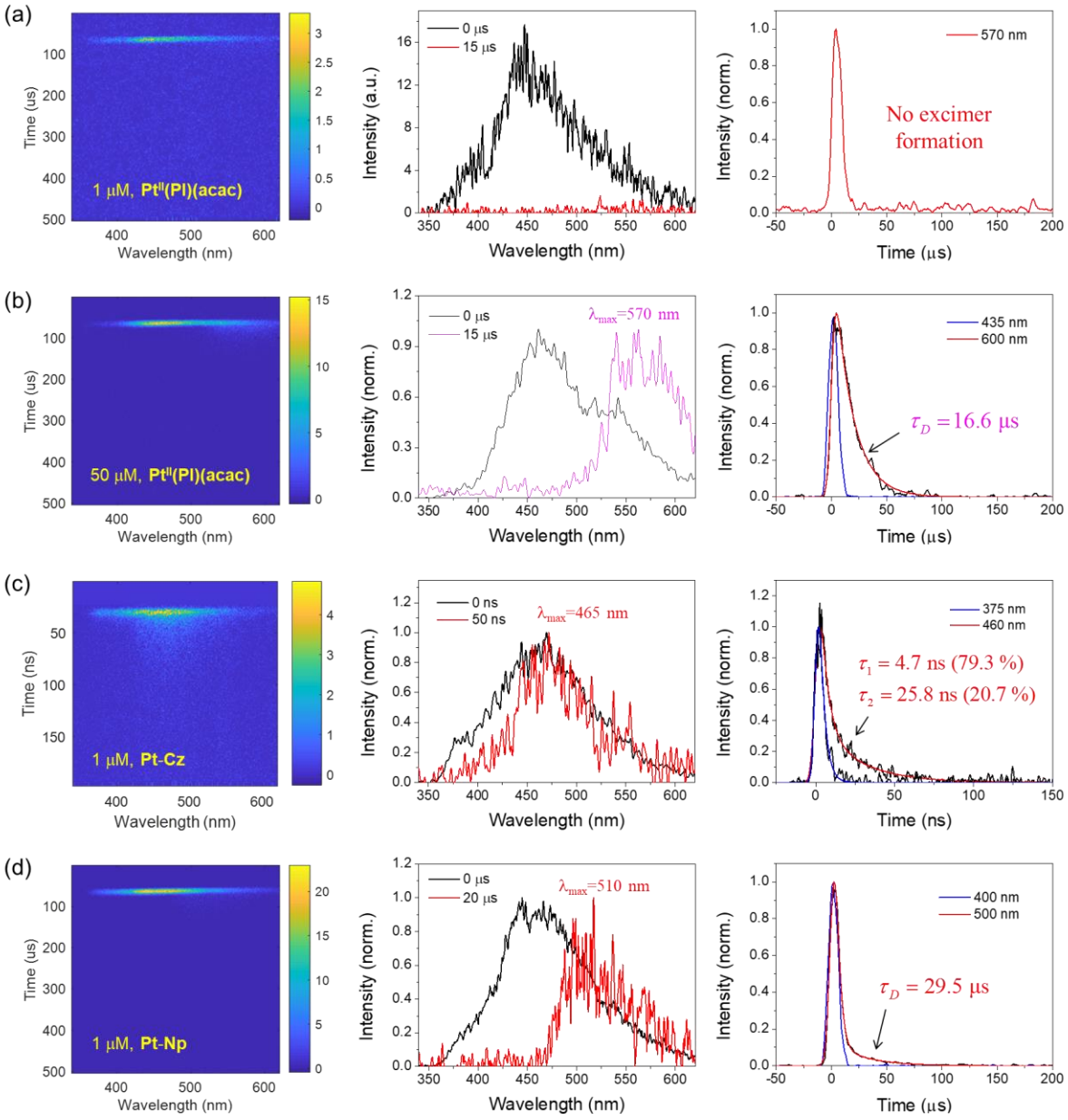

Supplementary Figure 11. Time-resolved photoluminescence (TRPL) spectra (raw contour image, left) of (a) Pt^{II}(PI)(acac) (1 μM), (b) Pt^{II}(PI)(acac) (50 μM), (c) **Pt-Cz** (1 μM), and (d) **Pt-Np** (1 μM) in DCM. The vertical colorbar represents the PL intensity in counts per second (cps). Two representative TRPL spectra at (middle), as well as two time-profiles at 400~500 nm (right), are presented. Multi-exponential fitting results of the TRPL profiles are summarized in **Supplementary Table 6**.

Supplementary Table 6. Multiexponential fitting results for the TRPL profiles of Pt^{II}(PI)(acac), **Pt-Cz**, and **Pt-Np** in DCM. In the detection wavelength (λ_{em}) column, the symbols T and E in parentheses denote TTET (^{3}LC) and excimer, respectively.

Sample	Conc. (μM)	λ_{em} (nm)	A_1 (%)	τ_1 (μs)	A_2 (%)	τ_2 (μs)
Pt^{II}(PI)(acac)	1	450	100	1.1		
Pt-Np	1	400	100	< IRF [a]		
		550 (T)	96.0	< IRF	4.0	29.5
Pt^{II}(PI)(acac)	50	435	100	< IRF		
		600 (E)			100	16.6
Pt-Cz	50	375	91.6	< IRF	8.4	23.9 ns
		465 (T)			100	24.2 ns
Pt-Np	50	400				
		475 (T)			100	>100 [b]
		600 (E)	-36.5 [c]	17.8	63.5	>100

a) This component is limited by the time-resolution (IRF width) of the streak-scope setup. b) The decay component longer than 100 μs is limited by the Ar-purging condition. c) Negative amplitude indicates a rise component.

Supplementary Table 7. Multiexponential fitting results for the TRPL profiles of Pt^{II}(PI)(acac), **Pt-Cz**, and **Pt-Np** in PMMA (5 wt%) and crystalline form. In the detection wavelength (λ_{em}) column, the symbols T and E in parentheses denote TTET (^{3}LC) and excimer, respectively.

Sample	Phase	λ_{em} (nm)	A_1 (%)	τ_1 (μs)	A_2 (%)	τ_2 (μs)	A_3 (%)	τ_3 (μs)
Pt^{II}(PI)(acac)	PMMA	450	53.8	1.01	46.2	3.41		
	Crystal	450	69.9	38 ns	25.3	176 ns	4.8	0.70
		600 (E)	79.4	1.14	16.9	27.8	3.8	52.2
Pt-Cz	PMMA	375	94.6	<IRF [a]	5.4	> 5		
		465 (T)	40.9	0.89	37.1	4.06	22.1	10.4
	Crystal	375	96.6	<IRF	3.4	> 0.5		
		465 (T)	77.1	30.6 ns	21.5	0.12	1.3	0.72
		550 (E)	48.4	1.50	46.9	6.90	4.6	26.2
Pt-Np	PMMA	475 (T)	57.4	1.17	39.1	3.84	3.5	19.4
		600 (E)	54.1	0.87	44.4	3.54	1.4 (0.3)	34.8 (230) [b]
	Crystal	475 (T)	48.3	0.24	30.8	9.1	20.9	16.7
		600 (E)	-33.8 [c]	1.82	36.8	10.0	29.4	16.0

a) This component is limited by the time-resolution (IRF width) of the streak-scope setup. b) at 600 nm, a negligible decay component of 230 μs (A = 0.3 %) was found in the extended time window of 500 μs. c) Negative amplitude indicates a rise component.

Q1-5. *In the methods of synthesis section, the data of ^{13}C NMR should be presented for the structure characterizations.*

A1-5. According to the reviewer's request, we have added the ^{13}C NMR characteristics of samples to the revised manuscript and supporting information.

Pt-Cz: Pt-Cz was prepared according to a modified literature procedure.[38] **CzPI$^+$** (0.7 g, 1.7 mmol) and silver oxide (Ag_2O, 0.2 g, 0.9 mmol) were dissolved in 1,4-dioxane (15 mL) and stirred for 16 h at room temperature. The mixture was then filtered using methanol (MeOH, 30 mL) followed by solvent removal under reduced pressure. The Ag-substituted compound (0.5 g, 0.6 mmol) and dichloro(1,5-cyclooctadiene)platinum(II) (Pt(COD)Cl_2, 0.5 g, 1.2 mmol) were dissolved in 2-ethoxyethanol (15 mL). The mixture was refluxed for 16 h at 130°C. After cooling and solvent evaporation, the platinized solid residue (Pt(CzPI)Cl_2) was used for the subsequent reaction without further purification.

Next, Pt(CzPI)Cl_2 (0.5 g, 0.9 mmol) was dissolved in dimethylformamide (DMF, 45 mL) and subjected to 15 minutes of N_2 bubbling. Potassium-*tert*-butoxide (*t*-BuOK, 0.4 g, 3.4 mmol) and 2,4-pentanedione (acetylacetone, 0.3 mL, 3.4 mmol) were then added, and the mixture was stirred for 16 h at room temperature, followed by refluxed at 100°C for 6 hours. After the reaction was completed, the residue was filtered with dichloromethane (DCM, 50 mL) and purified by column chromatography using dichloromethane (DCM) and *n*-hexane (Hx). The desired product (**Pt-Cz**) was obtained from recrystallization using DCM and Hx and dried to afford the product as a beige powder. Yield: 0.15 g (29%).

^{1}H NMR (DMSO-d_6, 400 MHz, δ): 8.25 (d, J = 7.8 Hz, 2H), 8.06 (d, J = 2.1 Hz, 1H), 7.64 (d, J = 2.1 Hz, 1H), 7.57 (d, J = 8.2 Hz, 1H), 7.46 (t, J = 7.6 Hz, 3H), 7.36 (d, J = 8.2 Hz, 2H), 7.29 (t, J = 7.3 Hz, 2H), 7.23 (d, J = 8.0 Hz, 1H), 5.56 (s, 1H), 4.05 (s, 3H), 1.96 (s, 3H), 1.80 (s, 3H) (Supplementary Figure 1).

^{13}C NMR (Dichloromethane-d_2, 400 MHz, δ): 28.1, 35.4, 102.4, 110.7, 111.4, 115.1, 119.9, 120.6, 121.9, 122.8, 123.5, 126.3, 130.6, 133.4, 142.0, 147.2, 166.9, 185.7. (Supplementary Figure 2).

ESI-MS (*m*/*z*): calcd for $C_{27}H_{23}N_3O_2Pt$: 616.1438, found [M + Na^+] : 638.1705 (Supplementary Figure 3)

Pt-Np: Pt-Np was synthesized following the same procedure as described above for **Pt-Cz**, except **NpPi$^+$** was used instead of **CzPI$^+$**. Yield: 0.10 g (19%).

^{1}H NMR (DMSO-d_6, 400 MHz, δ): 8.06 (d, J = 8.7 Hz, 1H), 8.03-7.96 (m, 2H), 7.93 (d, J = 1.0 Hz, 1H), 7.70 (d, J = 7.4 Hz, 1H), 7.61 (d, J = 3.9 Hz, 1H), 7.59 (d, J = 3.9 Hz, 1H), 7.49 (d, J = 8.3 Hz, 1H), 6.99 (d, J = 2.3 Hz, 1H), 6.98 (t, J = 7.6 Hz, 1H), 6.88 (d, J = 7.6 Hz, 1H), 5.94 (d, J = 2.3 Hz, 1H), 5.61 (s, 1H), 3.94 (s, 3H), 2.03 (s, 3H), 1.95 (s, 3H) (Supplementary Figure 4)

^{13}C NMR (Dichloromethane-d_2, 400 MHz, δ): 28.3, 35.3, 102.3, 118.4, 120.3, 123.8, 126.9, 127.2, 128.3, 128.4, 128.7, 131.2, 133.3, 133.9, 137.8, 144.8, 151.2, 185.8. (Supplementary Figure 5).

ESI-MS (*m*/*z*): calcd for $C_{25}H_{22}N_2O_2Pt$: 577.1329, found [M + Na^+] : 599.1312 (Supplementary Figure 6)

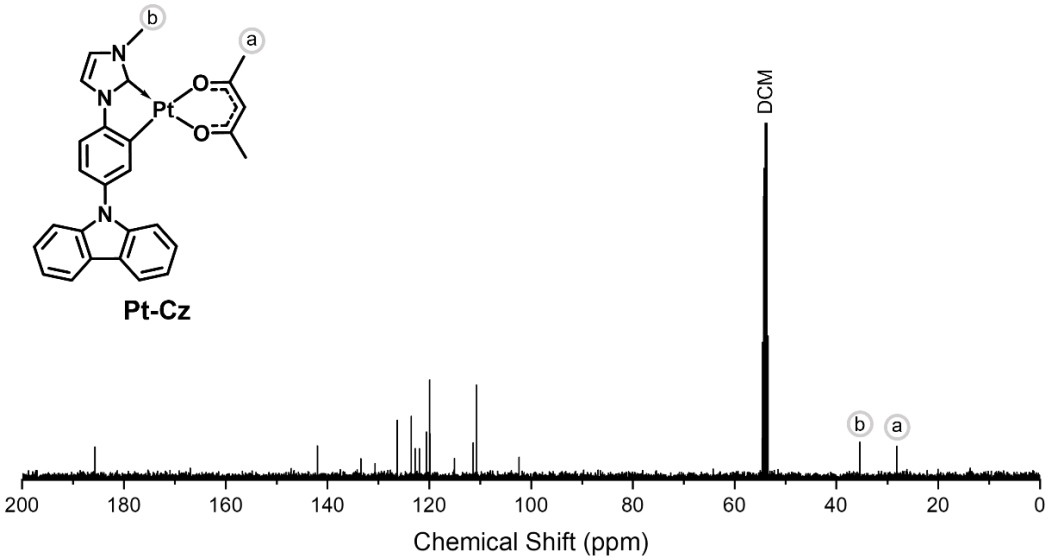

Supplementary Figure 2. ^{13}C-NMR of **Pt-Cz**.

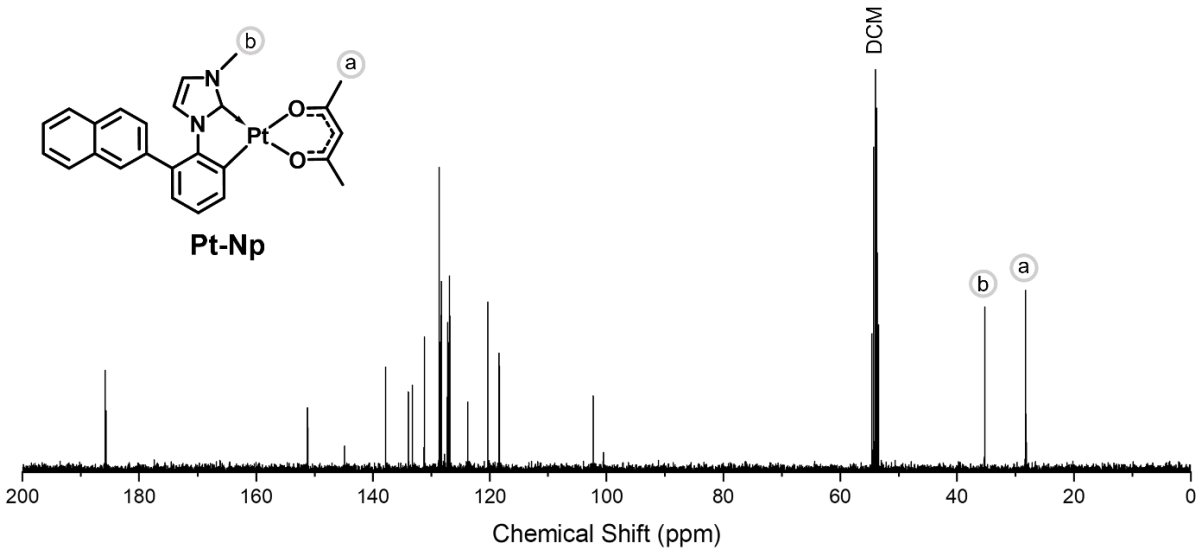

Supplementary Figure 5. ^{13}C-NMR of **Pt-Cz**.

Reviewer: 2

Comments: The authors, S. W. Jeong, H. J. Lee, T. Kim, C. H. Kim, H.-J. Son et al., reported on the novel four-coordinate N-heterocyclic carbene Pt(II) complexes bearing carbazole or naphthalene group showing exothermic triplet-triplet energy transfer, in particular persistent organic phosphorescence of organic molecules under ambient conditions. The results of this paper look like giving an insight to corresponding researcher for luminescent materials in both the academic and optoelectronic industrial fields. The approach for the purpose of this work was also well designed. The description for the Introduction section well focused on this research scoop and the added reference papers look proper. In this regard, the reviewer would like to recommend that the manuscript would be suitable for publication to Communications Chemistry as an Article. However, there are the parts which the authors should revise the manuscript and thoroughly consider as the following:

Q2-1. *Figure 1: It would be helpful to either indicate the dihedral angle or demonstrate the orthogonality between the ligand and substituent.*

A2-1. According to the reviewer's comment, we have updated Figure 1 to include the dihedral angle and show the orthogonality between the carbene ligand and organic tethers (see the revised Fig. 1a and 1b below).

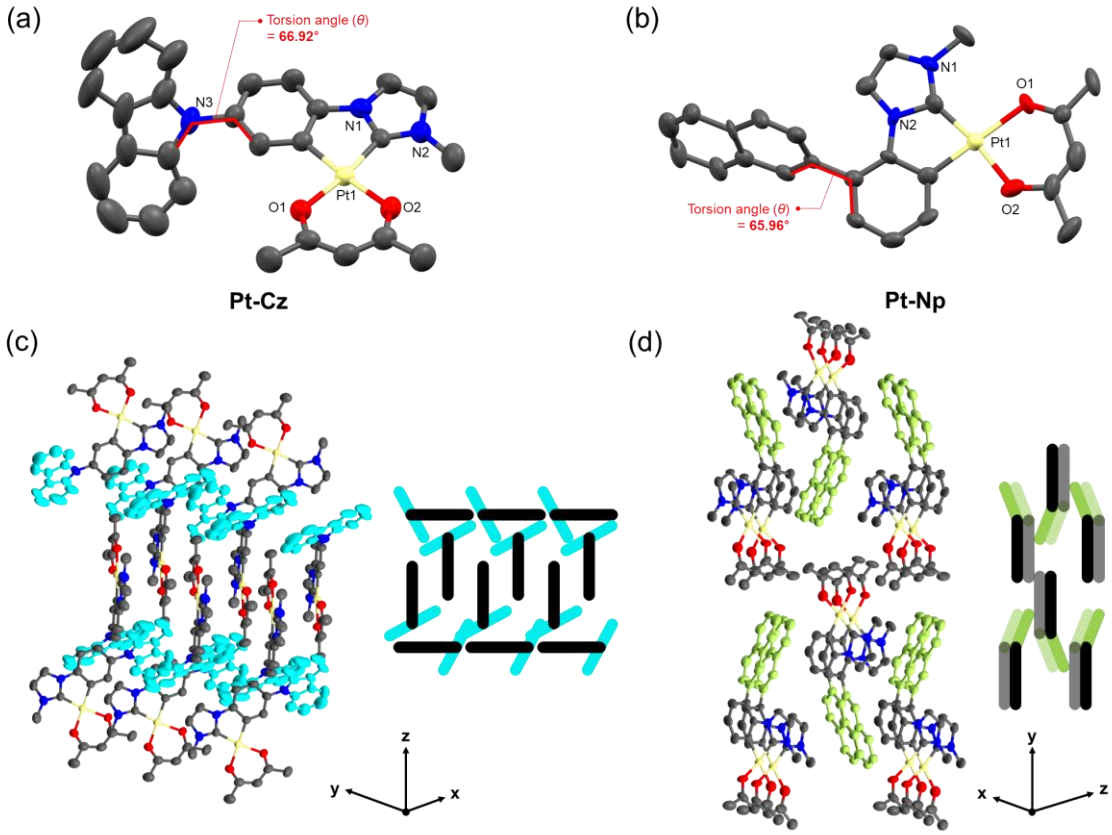

Fig. 1 X-ray crystal structures of (a) **Pt-Cz** and (b) **Pt-Np** with 30% probability for the thermal ellipsoids and packing diagram showing the intermolecular interaction of (c) **Pt-Cz** and (d) **Pt-Np**. Hydrogen atoms are omitted for clarity.

Q2-2. *Line #154: The text describes 312 nm, but Table 1 lists it as 313 nm. Harmonizing such numerical discrepancies would enhance readability. Review and correct similar instances throughout the manuscript if any.*

A2-2. Many thanks to reviewer's thoughtful comment. We have corrected all typos including the numerical discrepancy between Table 1 and the related text.

Q2-3. *Figure 3 (middle): The PL data for Pt^{II}(PI)(acac) + Cz and Pt^{II}(PI)(acac) + Np suggest fluorescence from Cz or Np and phosphorescence from Pt(II) (line #193 and #201). However, the graph shows a slight shoulder peak for Pt(PI)(acac) + Np, while phosphorescence is not convincingly observed for Pt(PI)(acac) + Cz. Please clarify this inconsistency.*

A2-3. In response to the reviewer's comment, we re-measured the PL spectra for the mixed sample (Pt^{II}(PI)(acac) + Np). The updated PL spectra has been added to the revised Figure 3 (see figure below). The phosphorescence peak of the Pt(II) complex in Pt^{II}(PI)(acac) + Cz is not observed because its intensity is much weaker than the fluorescence intensity of Cz, making it negligible in the spectra.

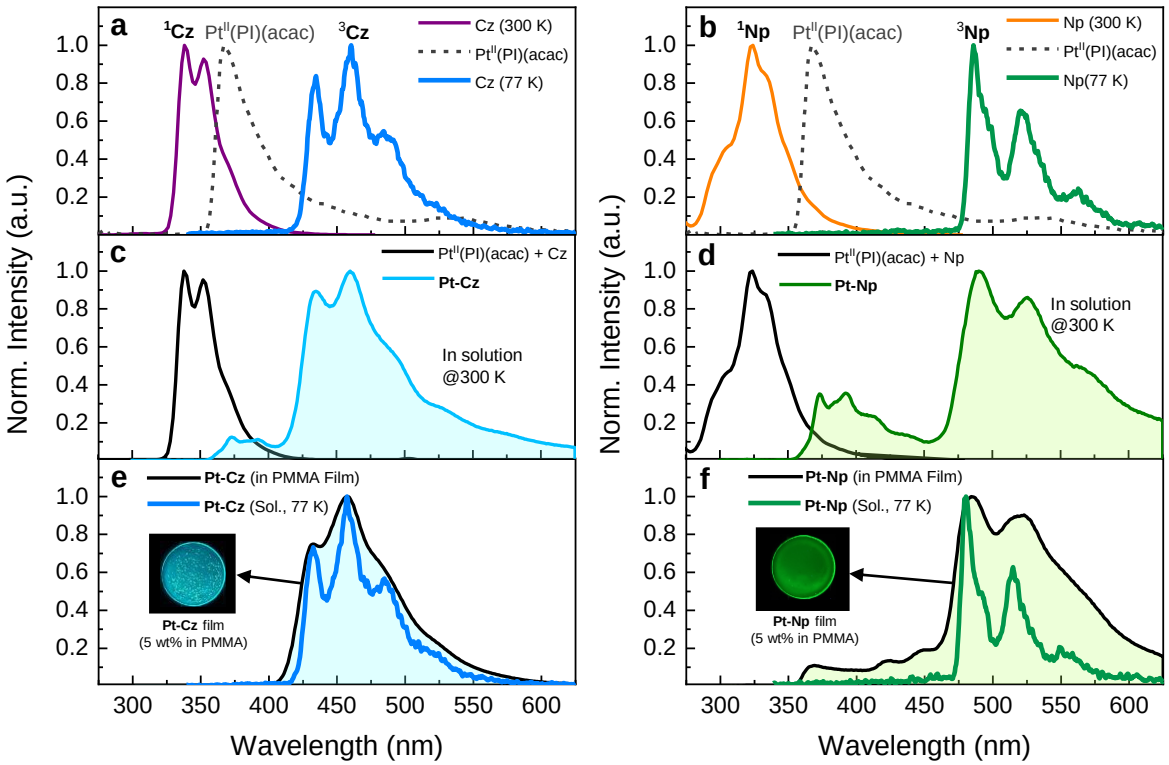

Fig. 3 Steady-state emission spectra (a and b) of Pt^{II}(PI)(acac), Cz, and Np (10 μM) recorded in DCM at 300 K and in 2-MeTHF at 77 K. Emission spectra (c and d) of **Pt-Cz** and **Pt-Np**, along with reference samples (Pt^{II}(PI)(acac) and organic tethers Cz and Np), obtained in DCM at 300 K. Emission spectra (e and f) of **Pt-Cz** and **Pt-Np** in PMMA films (5 wt% Pt(II) complex) at 300 K and in 2-MeTHF at 77 K.

Q2-4. *Line #236~: The statement that "the PL excitation spectra of both **Pt-Cz** and **Pt-Np** show distinct bands in the 340–400 nm range" does not align with the data in Supplementary Figure 8. Apart from **Pt-Cz**'s very weak absorption (λ_{em} = 450 nm, green line), no clear data supports this range. Please address this discrepancy.*

A2-4. We appreciate for reviewer's indication. According to reviewer's indication, we have revised the corresponding text. The corrected text reads "*the PL excitation spectra of both **Pt-Cz** and **Pt-Np** show distinct bands in the 280–350 nm range.*"

Q2-5. *Page 13, Line #251: The excimer emission is described as appearing at 50 μM, which seems unexpectedly dilute. While* ***Pt-Np****'s behavior at 1 μM is somewhat understandable, excimer emission attributed to Pt-Pt interaction (Line #251) suggests that* ***Pt-Cz*** *might also exhibit this phenomenon. Additional experiments, such as PL measurements at high concentrations (above mM) or in the crystalline state, could be helpful. Molecular interaction data from unit cell analyses of* ***Pt-Np*** *and* ***Pt-Cz*** *crystals would strengthen this discussion.*

A2-5. The crystal packing geometry of **Pt-Np** reveals stronger intermolecular interactions, arranged in a herringbone pattern, compared to **Pt-Cz** (see the revised Fig. 1c and 1d). These structural differences play a critical role in excimer formation and structural rigidity, significantly influencing the photophysical properties of Pt(II) complexes in highly concentrated solutions and solid-state environments. As expected, the photoluminescence (PL) spectra of **Pt-Np** at more than 50 μM show a red-shifted emission compared to the less concentrated solution (1–10 μM) (see figure below). This red shift highlights the strong intermolecular interactions that occur when **Pt-Np** molecules are in close proximity. Notably, the red-shifted PL emission at more than 200 μM closely resembles the emission observed in the crystalline state, confirming significant intermolecular interactions. In contrast, the PL spectra of **Pt-Cz** remain largely unchanged across a wide range of concentrations (1–50 μM in dilute solutions and 200 μM to 1 mM in concentrated ones), indicating weaker intermolecular interactions (see Supplementary Figure 12 below). However, in the crystalline state, **Pt-Cz** does show a red shift compared to its solution spectra, caused by molecular rigidification and solid-state interactions. These photophysical trends align with the differences in molecular interactions revealed by the crystal packing structures of **Pt-Np** and **Pt-Cz**."

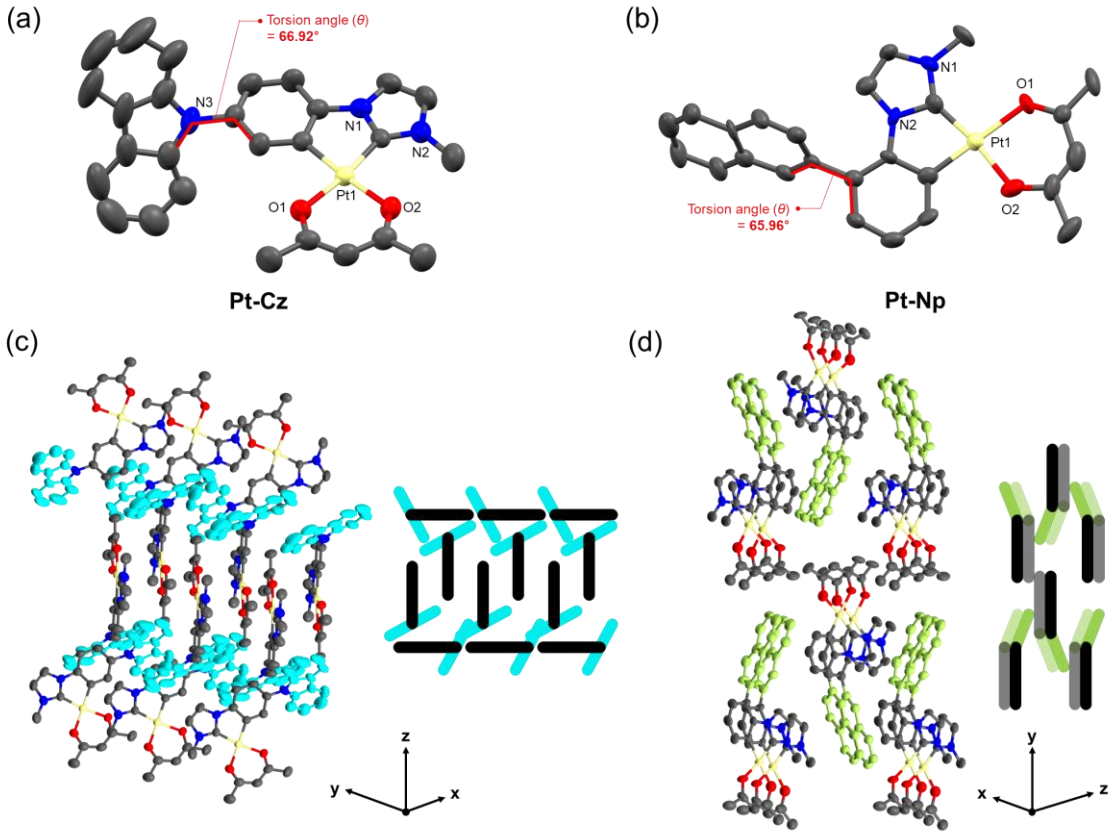

Fig. 1 X-ray crystal structures of (a) **Pt-Cz** and (b) **Pt-Np** with 30% probability for the thermal ellipsoids and packing diagram showing the intermolecular interaction of (c) **Pt-Cz** and (d) **Pt-Np**. Hydrogen atoms are omitted for clarity.

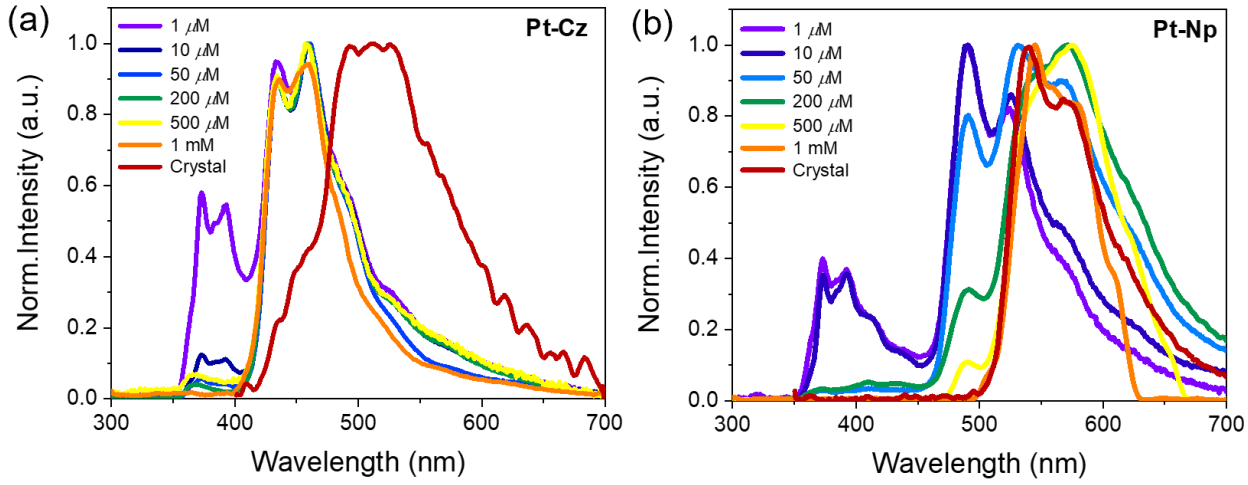

Supplementary Figure 12. Steady-state emission spectra of (a) **Pt-Cz** and (b) **Pt-Np** across a wide range of solution concentrations (1 μM to 1 mM) and in the crystalline state.

To address this, we have included additional discussion in the revised text (on pages 8 and 15-17):

The revised text reads "*It is noteworthy that, in comparison to **Pt-Cz**, the crystal packing geometry of **Pt-Np** exhibits stronger intermolecular interactions arranged in a herringbone pattern (Fig. 1d). This variation significantly influences the extent of excimer formation and the structural rigidity, thereby impacting the photophysical properties of Pt(II) complexes in highly concentrated solutions and solid-state environments (vide infra). (…) To systematically investigate the excimer formations of **Pt-Cz** and **Pt-Np** in solution, the steady-state PL spectra of the two samples were recorded with varying concentrations (1 μM ~ 1 mM) (Supplementary Figure 12). For comparison, steady-state PL spectra of their crystalline forms were also recorded to get insights into excimer formation in extended oligomeric aggregates. **Pt-Cz** solutions displayed nearly identical emission features around 465 nm (^{3}LC) with negligible excimer band at 570 nm across a wide concentration range (1 μM to 1 mM). The fully red-shifted excimer band was observed only in its crystalline state. The predominant generation of the ^{3}[Cz]* state in solution indicates that the perpendicular geometry of the appended Cz moiety effectively prevents intermolecular stacking interactions even in the highly concentrated solution (>50 μM). Consequently, the apparent red-shifted PL band by the ultrafast TTET process can be exclusively observed in **Pt-Cz,** as shown in Fig. 4c. On the other hand, the short PL lifetime of ~24 ns at 465 nm (see Supplementary Table 6) indicates that flexible skeletal motions of **Pt-Cz** in the excited state cause rapid non-radiative relaxations of the ^{3}[Cz]* state.[39] This is further supported by the prolonged PL lifetime of the ^{3}LC state in a glassy polymer matrix (vide infra). The strong intermolecular interactions in **Pt-Np** are further corroborated by the pronounced change in the excimer band with increasing concentration and its resemblance to the single PL band at 570 nm observed in the crystalline state. That is, the Np group plays a key role in inducing more rigid and extended H-type molecular aggregates in solution. In this context, the formation of the well-stacked aggregates should be responsible for the prolonged PL lifetimes (>100 μs) of both ^{3}LC and excimer states in the concentrated solution (50 μM) (Fig. 4f).*

Q2-6. *Page 13, Figure 4 & Supplementary Figure 9: The criteria for selecting the wavelengths for time-profile measurements are unclear. For example, Fig. 2 shows emission wavelengths corresponding to **Pt-Cz** and the excimer peak for 1 μM Pt^{II}(PI)(acac). However, other cases feature measurements at ambiguous wavelengths, such as near PL valleys. Consider either unifying the criteria or providing a clear explanation.*

A2-6. We chose the detection wavelengths to avoid the spectral overlap between the ^{3}LC and excimer emission bands. For example, in Fig. 4b, the PL lifetime of the excimer band at ~550 nm must be contaminated by the red-shoulder of the ^{3}LC emission. To avoid the reviewer's concern, added the symbols "T" and "E" to the detection wavelength column in Supplementary Tables 6-7 as follows.

Supplementary Table 6. Multiexponential fitting results for the TRPL profiles of Pt^{II}(PI)(acac), **Pt-Cz**, and **Pt-Np** in DCM. In the detection wavelength (λ_{em}) column, the symbols T and E in parentheses denote TTET (^{3}LC) and excimer, respectively.

Sample	Conc. (μM)	λ_{em} (nm)	A_1 (%)	τ_1 (μs)	A_2 (%)	τ_2 (μs)
Pt^{II}(PI)(acac)	1	450	100	1.1		
Pt-Np	1	400	100	< IRF [a]		
		550 (T)	96.0	< IRF	4.0	29.5
Pt^{II}(PI)(acac)	50	435	100	< IRF		
		600 (E)			100	16.6
Pt-Cz	50	375	91.6	< IRF	8.4	23.9 ns
		465 (T)			100	24.2 ns
Pt-Np	50	400				
		475 (T)			100	>100 [b]
		600 (E)	-36.5 [c]	17.8	63.5	>100

a) This component is limited by the time-resolution (IRF width) of the streak-scope setup. b) The decay component longer than 100 μs is limited by the Ar-purging condition. c) Negative amplitude indicates a rise component.

Supplementary Table 7. Multiexponential fitting results for the TRPL profiles of Pt^{II}(PI)(acac), **Pt-Cz**, and **Pt-Np** in PMMA (5 wt%) and crystalline form. In the detection wavelength (λ_{em}) column, the symbols T and E in parentheses denote TTET (^{3}LC) and excimer, respectively.

Sample	Phase	λ_{em} (nm)	A_1 (%)	τ_1 (μs)	A_2 (%)	τ_2 (μs)	A_3 (%)	τ_3 (μs)
Pt^{II}(PI)(acac)	PMMA	450	53.8	1.01	46.2	3.41		
	Crystal	450	69.9	38 ns	25.3	176 ns	4.8	0.70
		600 (E)	79.4	1.14	16.9	27.8	3.8	52.2
Pt-Cz	PMMA	375	94.6	<IRF [a]	5.4	> 5		
		465 (T)	40.9	0.89	37.1	4.06	22.1	10.4
	Crystal	375	96.6	<IRF	3.4	> 0.5		
		465 (T)	77.1	30.6 ns	21.5	0.12	1.3	0.72
		550 (E)	48.4	1.50	46.9	6.90	4.6	26.2
Pt-Np	PMMA	475 (T)	57.4	1.17	39.1	3.84	3.5	19.4
		600 (E)	54.1	0.87	44.4	3.54	1.4 (0.3)	34.8 (230) [b]
	Crystal	475 (T)	48.3	0.24	30.8	9.1	20.9	16.7
		600 (E)	-33.8 [c]	1.82	36.8	10.0	29.4	16.0

a) This component is limited by the time-resolution (IRF width) of the streak-scope setup. b) at 600 nm, a negligible decay component of 230 μs (A = 0.3 %) was found in the extended time window of 500 μs. c) Negative amplitude indicates a rise component.

Q2-7. *Figure 4 (top): Include an explanation of the data, and clarify the meaning of the blue-to-yellow color gradient with appropriate labels.*

A2-7. According to the reviewer's comment, we have added the explanation for Fig. 4a and 4b to the revised text with adding labels for the blue-to-yellow color gradient (see the revised Fig. 4).

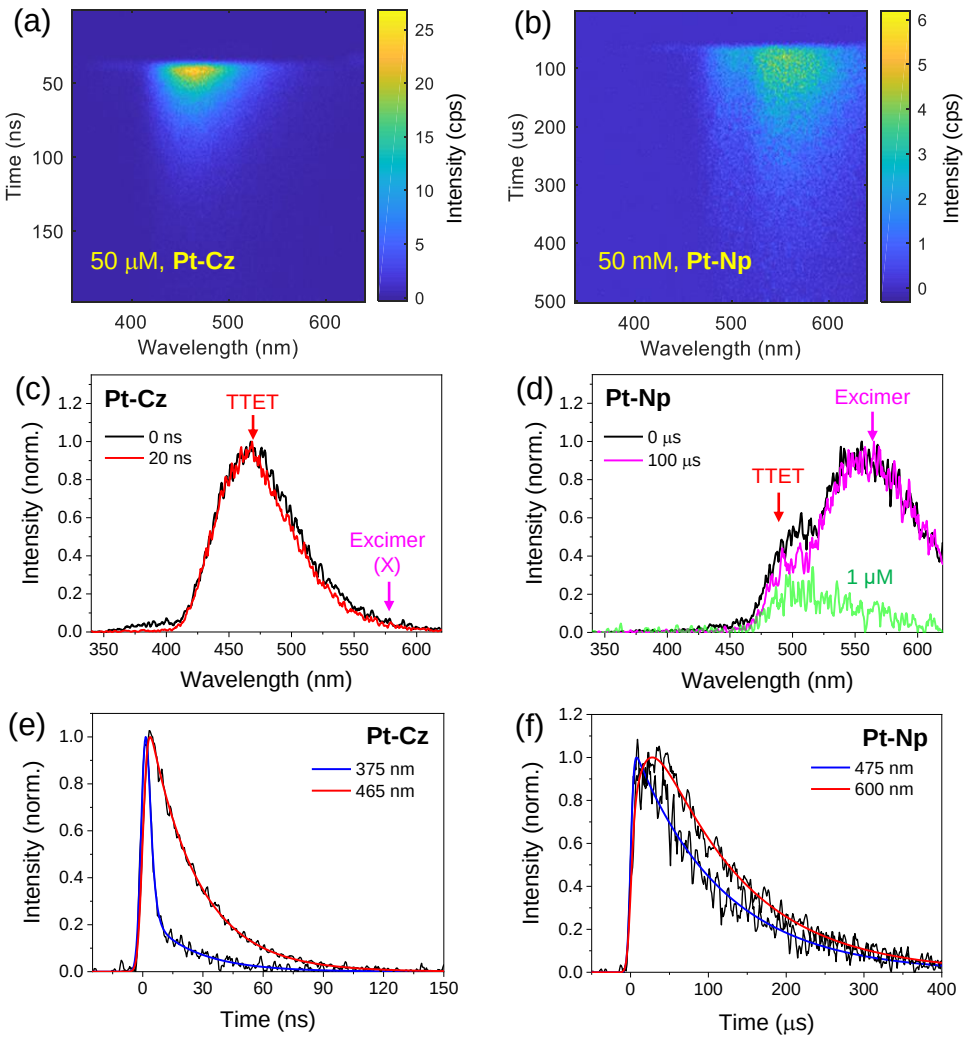

Fig 4. Time-resolved photoluminescence (TRPL) spectra (raw contour images, top) of (a) **Pt-Cz** and (b) **Pt-Np** in DCM (50 μM), where the vertical colorbar (right) represents the PL intensity in counts per second (cps). For comparison, the TRPL spectra obtained at two representative time-delays (c and d) and the PL spectrum of the highly diluted **Pt-Np** solution (1 μM) was overlaid (green curve). The TRPL profiles for the blue and red spectral regions (e and f) are presented, and their multi-exponential fitting results are listed in Supplementary Table 6.

Q2-8. *Page 25, Supplementary Table 7: The increase in CIEy and EL emission wavelengths with higher dopant concentrations seems related to* ***Pt-Cz*** *excimer formation, as discussed in Line #452. This aligns with the questions #5, suggesting the need for additional experiments.*

A2-8. As noted by the reviewer, there is a clear relationship between dopant concentration in the emitting layer and the electroluminescence (EL) emission wavelength. This suggests that increased dopant concentration of **Pt-Cz** in the emitting layer leads to stronger intermolecular interactions, as the molecules are brought closer together. This is supported by the red-shift observed in the photoluminescence (PL) emission of the crystalline state compared to a wide range of solution concentrations. Additionally, the similarity between the EL spectrum of the 15%-doped device and the steady-state PL spectrum in the crystalline state further supports this inference (see figure below). However, confirming the presence of excimer formation in the EL device remains challenging at this time. In-situ photodynamic analysis is hindered by significant scattering and photodamage of the solid samples during measurements. We plan to address this limitation in a future study with an improved measurement setup.

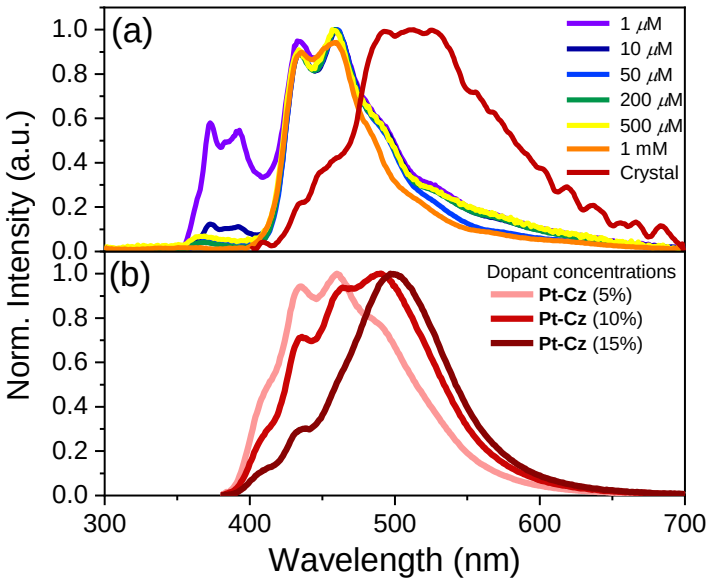

Supplementary Figure 19. (a) Steady-state emission spectra of **Pt-Cz** measured at various solution concentrations (1 μM to 1 mM) and in its crystalline form and (b) electroluminescence spectra of a **Pt-Cz**-doped device with dopant concentrations of 5%, 10%, and 15%.

Q2-9. *Thermal stability: Since device testing was performed, additional TGA experiments to analyze thermal stability and decomposition characteristics would be beneficial.*

A2-9. According to the reviewer's request, we have added the TGA data for **Pt-Cz** and **Pt-Np** to the revised SI (see figure below).

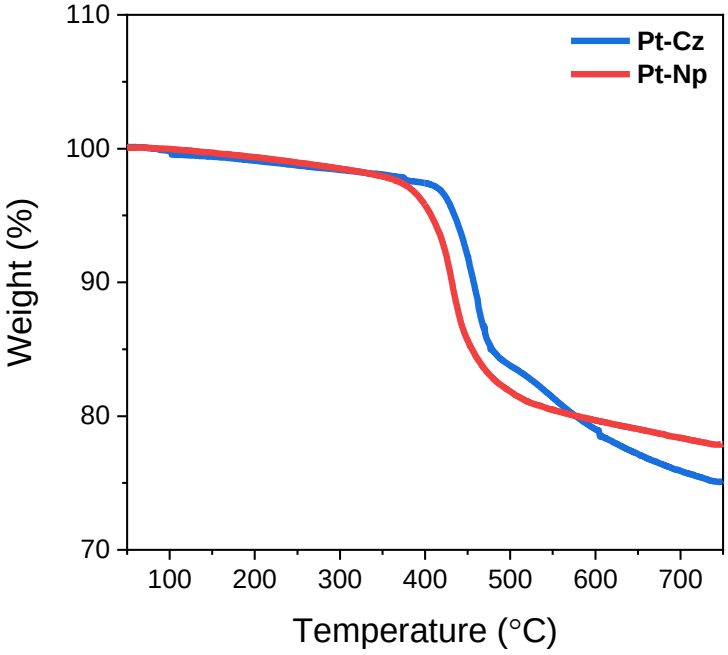

Supplementary Figure 20. Thermogravimetric analysis (TGA) curves and parameters of **Pt-Cz** and **Pt-Np**. TGA was recorded on a Perkin-Elmer TGA 4000 instrument in the temperature range of 30 to 800 °C under N_2 flow, with a heating rate of 30 °C min^{-1}.

Q2-10. *Figures 8 & 2: The absorption spectra in Fig. 2 suggest that* ***Pt-Cz****'s vertical excitation is similar to Cz, while* ***Pt-Np*** *resembles Pt(II). This implies that Fig. 8a's vertical excitation for* ***Pt-Cz*** *might terminate at* ^{1}*[Cz]* rather than* ^{1}*MLCT. What is the authors' perspective on this?*

A2-10. The similarity between Cz and **Pt-Cz** occurs because the Cz unit has a much stronger intensity compared to the Pt(II) complex. In contrast, the absorption spectra of **Pt-Np** are similar to the Pt(II) complex because the Np unit has a weaker intensity than the Pt(II) core complex.

Q2-11. *Figure 8: Despite both molecules having the same TTET mechanism, the final emission lifetimes differ significantly (24 ns vs. >100 μs). A more detailed explanation is needed for this discrepancy. Is there any some examples previously reported?*

A2-11. As detailed in the response *Q2*-5 to Reviewer 2, the intermolecular interactions of **Pt-Np** in solution are stronger than those of **Pt-Cz** in solution. The dense packing of **Pt-Np** in herringbone modes suppresses intramolecular skeletal motions, resulting in the significant increase in photoluminescence (PL) lifetime. This observation aligns with previously reported studies showing an extended phosphorescence lifetime (~100 ms) in well-packed Cz-containing OPRTP materials (Tang et al. *Nat. Commun.* **10**, 1595 (2019)). We have incorporated this discussion into the revised text (on page 18-19), which now reads: "*The excited state dynamics of* ***Pt-Np*** *in condensed phase was highly complicated by the formation of molecular aggregates facilitated by the organic tether moieties (Supplementary Figures 13-14 and Tables 6-7). As shown in Fig. 4d, the* ***Pt-Np*** *solution revealed the strong* ^{3}*LC and excimer emissions due to effective stacking interactions in the aggregates. Notably, the PL lifetimes of both* ^{3}*LC and excimer states were rather longest (>100 μs) in the concentrated solution (50 μM) than in the crystalline form. In the crystal, the PL lifetime of the* ^{3}*LC state at 475 nm was ~250 ns, while the 2*nd *and 3*rd *time constants (10~16 μs) were attributed to spectral overlap of the strong excimer emission at 600 nm. This is in sharp contrast to* ***Pt-Cz****, where the* ^{3}*[Cz]* product in solution undergoes the relatively fast deactivation (~24 ns) compared to that in the solid-state samples. According to the packing structure of* ***Pt-Np*** *crystal in Fig. 1d, the herringbone arrangements of fully-stacked* ***Pt-Np*** *dimeric units in the crystal may impede strong excitonic interactions across the extended spatial domain. In this context, we argue that extended H-type molecular aggregates with a long coherence length are favorable in solution, thereby reducing oscillator strengths of the optical transitions and suppressing structural distortions. It is noteworthy that the spectral width of the excimer PL band at 570 nm gradually decreased with increasing concentration (Supplementary Figure 12b), implying that effective and extended stacking interactions in solution promote the formation of a well-ordered aggregate with reduced conformational disorder. On the other hand, in the PMMA film (5 wt%), the PL lifetime at 475 nm was similar to that at 600 nm, and only an extremely weak PL with a time-constant of 230 μs was detected at 600 nm (Supplementary Table 7), indicating negligible excimer emission. Again, this confirms that the dopant concentration of 5 wt% is sufficiently low to minimize excimer formation in the thin film.*".

Q2-12. *Molecular design: Cz is located at the para position of phenyl, while Np is at the ortho position. Since the electronic environments differ, provide an explanation of the rationale and implications of these molecular designs.*

A2-12. Thank you for the reviewer's insightful comment. Initially, we synthesized three **Pt-Cz** complexes with Cz substitutions at the *ortho*-, *meta*-, and *para*-positions of the phenyl group. By comparing their TTET efficiencies through PL spectra, we identified the *para*-substituted **Pt-Cz** as the most efficient isomer. Therefore, we selected the *para*-substituted **Pt-Cz** for this study. We plan to explore the substitution dependency further in a future study with detailed photodynamic analysis.

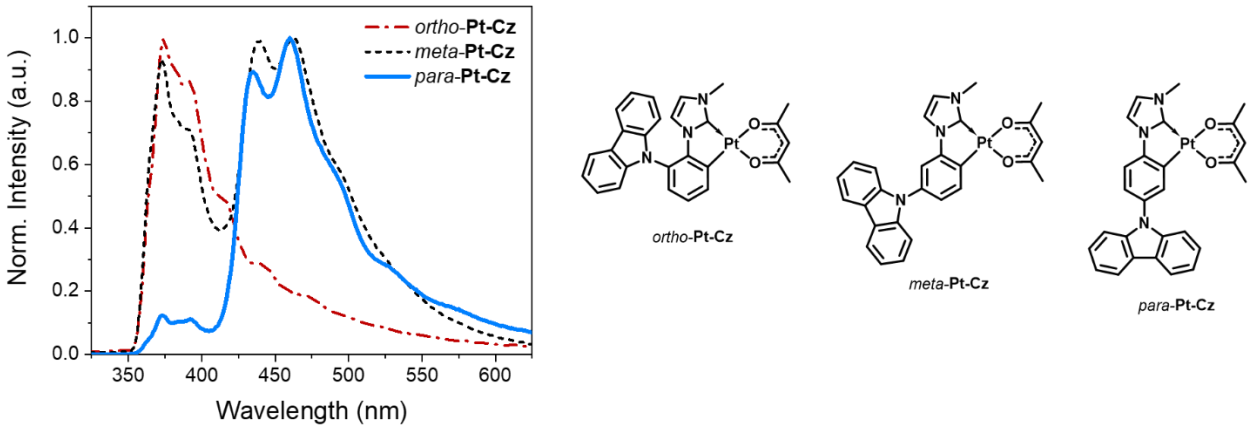

Fig. Steady-state emission spectra of *ortho*-**Pt-Cz**, *meta*-**Pt-Cz**, and *para*-**Pt-Cz** (10 μM) obtained in DCM at 300 K.

Q2-13. *Figure and Table descriptions: The explanations for figures and tables are insufficiently detailed, making it difficult to connect them with the text. Use clear symbols (a, b, etc.), and add detailed descriptors such as left, right, middle, top, and bottom in figure legends to enhance clarity.*

A2-13. According to the reviewer's request, we have revised the descriptions for figures and tables.

Q2-14. *The originality of this study, Line #69~: While the need for developing novel OPRTP materials without SOC via heavy atom effects is acknowledged, the manuscript ultimately relies on Pt to utilize SOC for TTET. This raises a question about the novelty of the approach. Address this concern.*

A2-14. This paper introduces a novel approach to achieving organic phosphorescence at the molecular level, rather than in the condensed phase, using a Pt(II) complex containing a heavy atom. While the Pt(II) complex plays a significant role, there are no prior examples of pure organic phosphorescence originating from carbazole (Cz) or Np units. Most existing OPRTP materials without SOC typically show red-shifted, broad emission bands caused by intermolecular interactions and condensed-phase characteristics, which differ from the independent properties observed in their low-temperature solution phosphorescence. Our study focuses on achieving phosphorescence from a single Cz unit and investigating its electroluminescent properties in OLEDs.

Minor points:
- Supplementary Scheme 1: Replace (v) with (iv) in the explanation section.
- Supplementary Figures 9 and 10: The concentration unit is incorrect; revise from mM to μM.
- Line #219: The footnote in Table 1 mentions 3 wt% PMMA, whereas the text specifies 5 wt%. Provide a clear and consistent description.

A. Thank you for pointing out the typos. We have corrected them accordingly.